Original Article

Clin Shoulder Elbow 2023;26(2):131-139
https://doi.org/10.5397/cise.2022.01207

CiSE
Clinics in Shoulder and Elbow

eISSN 2288-8721

Effect of suprascapular nerve injury on muscle and regenerated enthesis in a rat rotator cuff tear model

Kenichiro Eshima[1], Hiroki Ohzono[2], Masafumi Gotoh[2], Hisao Shimokobe[1], Koji Tanaka[1], Hidehiro Nakamura[2], Tomonoshin Kanazawa[1], Takahiro Okawa[2], Naoto Shiba[1]

[1]*Department of Orthopedic Surgery, Kurume University Hospital, Fukuoka, Japan*
[2]*Department of Orthopedic Surgery, Kurume University Medical Center, Fukuoka, Japan*

Background: Massive rotator cuff tears (RCTs) are complicated by muscle atrophy, fibrosis, and intramuscular fatty degeneration, which are associated with postoperative tendon-to-bone healing failure and poor clinical outcomes. We evaluated muscle and enthesis changes in large tears with or without suprascapular nerve (SN) injury in a rat model.
Methods: Sixty-two adult Sprague-Dawley rats were divided into SN injury (+) and SN injury (–) groups (n=31 each), comprising tendon (supraspinatus [SSP]/infraspinatus [ISP]) and nerve resection and tendon resection only cases, respectively. Muscle weight measurement, histological evaluation, and biomechanical testing were performed 4, 8, and 12 weeks postoperatively. Ultrastructural analysis with block face imaging was performed 8 weeks postoperatively.
Results: SSP/ISP muscles in the SN injury (+) group appeared atrophic, with increased fatty tissue and decreased muscle weight, compared to those in the control and SN injury (–) groups. Immunoreactivity was only positive in the SN injury (+) group. Myofibril arrangement irregularity and mitochondrial swelling severity, along with number of fatty cells, were higher in the SN injury (+) group than in the SN injury (–) group. The bone-tendon junction enthesis was firm in the SN injury (–) group; this was atrophic and thinner in the SN injury (+) group, with decreased cell density and immature fibrocartilage. Mechanically, the tendon–bone insertion was significantly weaker in the SN injury (+) group than in the control and SN injury (+) groups.
Conclusions: In clinical settings, SN injury may cause severe fatty changes and inhibition of postoperative tendon healing in large RCTs.
Level of evidence: Level Basic research, controlled laboratory study.

Keywords: Suprascapular nerve injury; Bone-tendon interface healing; Rotator cuff tear

INTRODUCTION

Generally, arthroscopic rotator cuff (RC) repair produces acceptable clinical outcomes [1]. However, the repair of chronic massive rotator cuff tears (RCTs) remains challenging, with a high structural failure rate of 34%–94% [2]. Ladermann et al. [3] reported that re-tear rates of massive RCTs reach as high as 80% because of tendon retraction, muscle atrophy, fatty infiltration, and osteoporosis. Choi et al. [4] found that the re-tear rate of massive RCTs was 53.3% (8/15 patients), and preoperative fatty degeneration was significantly more common in these patients than in those with an intact tendon after surgery.

Massive RCTs are complicated by muscle atrophy, fibrosis, and intramuscular fatty degeneration. These factors are associated with the failure of tendon-to-bone healing after surgery and eventually lead to worse clinical outcomes [5,6]. Matsumoto et al.

Received: August 17, 2022 Revised: November 22, 2022 Accepted: December 8, 2022
Correspondence to: Hiroki Ohzono
Department of Orthopedic Surgery, Kurume University Medical Center, 155-1 Kokubu-machi, Kurume, Fukuoka 839-0863, Japan
Tel: +81-942-22-6111, Fax: +81-942-22-6657, E-mail: ohzono_hiroki@kurume-u.ac.jp, ORCID: https://orcid.org/0000-0001-7170-5401

[7] reported that delayed tendon reattachment does not reverse atrophy or fat accumulation of the supraspinatus (SSP). Uhthoff et al. [8] reported that muscle atrophy and fat accumulation occur early after SSP tendon tear and immediate repair and found that early repair does not prevent fat accumulation. In fact, muscle atrophy and intramuscular fat accumulation occasionally occur after massive RCT in the clinical setting [9-11]. Although muscle atrophy and intramuscular fat accumulation are thought to be major factors that impair tendon-to-bone healing after RC repair, the underlying mechanisms remain unknown.

Previous studies have indicated a significant association between suprascapular nerve (SN) injury, muscle atrophy, and fatty degeneration in RCTs [12,13]. Shi et al. [13] reported that suprascapular neuropathy is correlated with tendon tear size, delayed SSP–nerve conduction velocity latency, and SSP fatty degeneration. Several researchers have identified a relationship between SN injury and RCT. Sasaki et al. [14] reported the results of histological and biomechanical examinations in rat models and suggested that the etiology of fatty infiltration after massive RCTs might be different from that of SN injury. In a massive RCT rodent model that included RCT transections, Liu et al. [15] observed significant denervation, consistent atrophy, and fat infiltration. In fresh-frozen cadavers, Albritton et al. [16] reported that the degree of RC muscle atrophy frequently observed after a massive tear may be explained by increased tension on the nerve due to muscle retraction. Taken together, these results suggest an association between muscle atrophy, intramuscular fat accumulation, and SN injury. Therefore, the purpose of the present study was to investigate the effects of SN injury on muscle changes in a massive RCT rat model, further extending the literature on enthesis alterations.

METHODS

The study was conducted according to the National Institute of Health's guidelines for animal research and was approved by the animal studies and the Institutional Animal Care and Use Committees of Kurume University Hospital (No. 2018-083). This study also received approval from the Ethics Review Board of the animal care center at Kurume University Hospital (No. 2019285). All efforts were made to minimize the number of animals used and their suffering.

Study Design

A total of 62 adult Sprague-Dawley rats (mean body weight, 334.5 ± 25.8 g) were divided into the following two groups: an SN injury (+) group (n = 31), which included both tendon and nerve resection cases, and an SN injury (–) group (n = 31), which included tendon resection–only cases. The operative side was randomly selected, and the opposite side on which a cuff tear was not made was used as a control. Each group was evaluated at 4, 8, and 12 weeks after surgery; at 4 and 12 weeks, we used seven rats for biomechanical testing and three rats for histology, while at 8 weeks, we used seven rats for biomechanical testing, three rats for histology, and one rat for ultrastructural analysis. At each time point, measurement of the SSP and infraspinatus (ISP) weights, histological analysis, and biomechanical testing were completed. Additionally, ultrastructural analysis with block face imaging was performed at 8 weeks after surgery (Fig. 1).

Surgical Procedure

All rats were treated according to the guidelines of the relevant institutional animal care and use committee. Each rat was anesthetized with isoflurane under a high flow rate of oxygen. Then, a middle longitudinal skin incision was made, and the subcutaneous tissue was divided to expose the deltoid. After exposure of the SSP tendon, the tendon insertion was detached and resected using a #11 scalpel blade, and the cartilaginous portion was protected at its insertion in the SN injury (–) group. Conversely, in the SN injury (+) group, the SN was dissected using microsurgical scissors just anterior to the suprascapular notch. The wound was then closed layer by layer and the animals were allowed to move freely in their cages after the operation. This surgical protocol was performed similarly to that described in a previous report (Fig. 2) [17].

Histological Analysis

Axial sections measuring 5 μm thick at the muscle belly (SSP) were processed for frozen sections and stained with hematoxylin and eosin and Oil Red O staining. To observe fatty tissue, the fixed specimens were frozen shortly with iced 99.5% ethanol and cut axially into 10-μm-thick sections. The specimens were visualized under a light microscope (BZ-X710, Keyence), and photomicrographs were obtained. Muscle atrophy was identified by a few suggestive findings, such as an angular shape of muscle fibers rather than a round shape, a reduced distance between myonuclei, and centralization of the myonuclei [17,18]. The muscle fiber size was not measured.

Ultrastructural Analysis Using Block Face Imaging

For each time point, rats were anesthetized with diethyl ether and sodium pentobarbital, which was transcardially perfused through the left ventricle with heparin-containing saline, and then fixed in half Karnovsky solution (2% paraformaldehyde,

https://doi.org/10.5397/cise.2022.01207

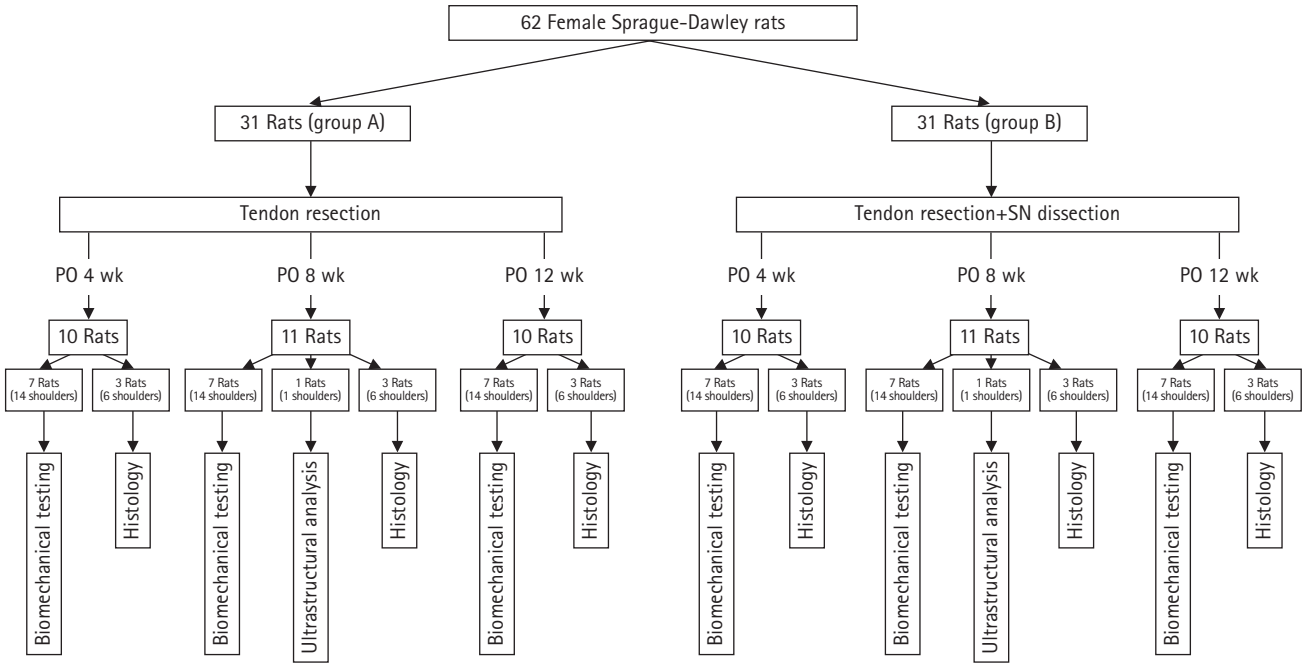

Fig. 1. Flow diagram of the study design illustrating how the rats were divided into groups for the three time points. PO: postoperative, SN: suprascapular nerve.

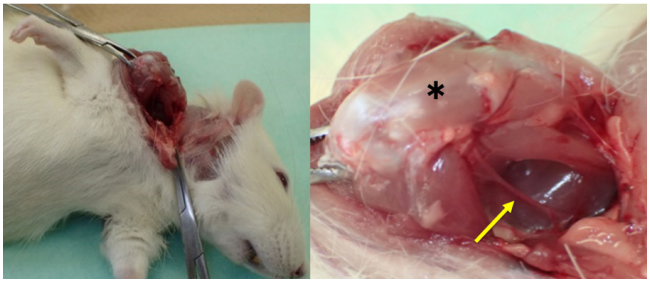

Fig. 2. Surgical procedure. The asterisk indicates the supraspinatus and the yellow arrow indicates the suprascapular nerve.

2.5% glutaraldehyde, and 2 mM of CaCl2 in a 0.1-M cacodylate buffer). The specimens were further immersed in the same fixative, then cut and further fixed with ferrocyanide and 1% osmium tetroxide (OsO_4). Subsequently, the specimens were treated with 1% thiocarbohydrazide and immersed in a 1% OsO_4 solution. For *en bloc* staining, the specimens were immersed in a solution of 4% uranyl acetate solution overnight and washed with distilled water. The specimens were further stained with Walton's lead aspartate solution and dehydrated with a graded ethanol series, infiltrated with an epoxy resin mixture, and polymerized at 60 °C for 72 hours. The surface of each embedded specimen was exposed with a diamond knife, and the resin blocks were trimmed and placed on an appropriate holder. Each specimen was fixed to the stage of the focused ion beam/scanning electron microscopy machine (Quanta 3DFEG, FEI). Block face images were acquired by image acquisition using scanning electron microscope for a compositional contrast image from secondary electrons.

Mechanical Testing at the Tendon–Bone Insertion Point

All specimens selected for biomechanical testing were dissected and stored at −80 °C. Specimens were thawed the day before biomechanical testing. Soft tissues over the humerus, except for the SSP tendon–humerus complex, were removed. The SSP tendon was secured in a screw grip using sandpaper and ethyl cyanoacrylate. All specimens indicated for biomechanical testing underwent micro–computed tomography (CT) imaging (R-mCT2, Rigaku Corp.) before testing, which was performed on the day of biomechanical testing with the specimens in saline. Each sample was placed in the holder and scanned at 90 kV and 160 μA. Following micro-CT scanning, the specimens were placed into a tensile testing machine (TENSILON RTE-1210, Orientec). The humerus was secured in a custom-designed pod using a capping compound, and the SSP tendon–humerus complex was positioned to allow tensile loading in the longitudinal direction of the SSP tendon–humerus interface. The specimens were preloaded to 0.1 N for 5 minutes, which was followed by five cycles of loading and unloading at a cross-head speed of 5 mm/min; then, they were loaded to failure at a rate of 1 mm/min and assessed for mechanical properties. Failure modes were recorded for each specimen. The ultimate load-to-failure was recorded for the peak load.

Linear stiffness was calculated by determining the slope of the linear portion of the load-elongation curve. Ultimate stress was calculated by dividing the ultimate load-to-failure by the cross-sectional area of the repaired tendon–bone interface, which was obtained from the axial section of the micro-CT image. Young's modulus was calculated by determining the slope of the linear portion of the stress–strain curve. The strain was calculated by dividing the elongation by the initial length obtained from the coronal section of the micro-CT image. This testing protocol was similar to that described previously [12].

Statistical Analysis

Statistical analysis was performed using JMP ver. 15 (SAS Institute Inc.). The Mann-Whitney U-test was used to compare the SN injury (+), SN injury (−), and control groups at each time point by comparing the weights of the SSP and ISP along with their mechanical properties. Statistical significance was set at $P < 0.05$. The Holm-Bonferroni sequential correction method was used to adjust P-values for multiple comparisons. Data are expressed as mean and standard deviation values.

RESULTS

Macroscopic Appearance

The appearance of the SSP and ISP muscles in the SN injury (−) group was similar to that of muscles on the non-operated side in the same group. On the contrary, in the SN injury (+) group, the muscles' appearance became atrophic throughout the study period compared to those on the non-operated side. No apparent increase in fatty tissue was observed in either group. Representative data are shown in Fig. 3A and B.

Average muscle weights of the SSP in the control, SN injury (+), and SN injury (−) groups were 1.52, 1.15, and 1.36 g at 4 weeks; 1.65, 1.15, and 1.46 g at 8 weeks; and 1.66, 1.20, and 1.64 g at 12 weeks, respectively. For ISP, average weights in the control, SN injury (+), and SN injury (−) groups were 1.43, 1.14, and 1.45 g at 4 weeks; 1.61, 1.25, and 1.56 g at 8 weeks; and 1.70, 1.26, 1.69 g at 12 weeks respectively. Details are shown in Fig. 3C and D. Differences with $P < 0.05$ were considered statistically significant.

Histological Analysis

In the SN injury (−) group, muscle fibers were slightly atrophic with regular nuclear arrangement. These changes were similar throughout the experiment periods (Fig. 4A-C). In contrast, in the SN injury (+) group, the muscle fibers showed more advanced atrophy with irregular nuclear arrangement, and the changes became remarkable in the elapsed periods (Fig. 4D-F). Following Oil Red O staining, there were no positive immunoreactivities at any time point in the SN injury (−) group (Fig. 5A-C). In the SN injury (+) group, the immunoreactivity was negative at 4 weeks but positive at 8 and 12 weeks after surgery; in other words, the immunoreactivity between the muscle fibers was enhanced gradually (Fig. 5D-F).

Ultrastructural Analysis

For ultrastructural analysis, 8-week specimens were used. In the SN injury (−) group, myofibril arrangement appeared to be slightly irregular with mild swelling of the mitochondria compared to that on the nonoperative side in the same group. There were no fatty cells in the myofibril or inter-myofibril space. On the other hand, the myofibril arrangement and extent of mitochondrial swelling in the SN injury (+) group were more irregular and severe compared to those in the SN injury (−) group. Moreover, fatty cells were often seen around the myofibril border. Representative data are shown in Fig. 6.

Histology at the Tendon–Bone Insertion Point

The bone–tendon junction was reconstructed using granulation tissue in both groups. In the SN injury (−) group, a firm enthesis was seen, including dense mature fibrocartilage and well-aligned cells. In the SN injury (+) group, the enthesis was relatively atrophic and thinner with decreased cell density and immature fibrocartilage (Fig. 7).

Mechanical Properties at the Tendon–Bone Insertion Point

The mean ultimate stress was 4.13, 0.56, 2.32 MPa at 4 weeks ($P < 0.05$); 4.58, 0.29, 0.70 MPa at 8 weeks ($P < 0.05$); and 3.14, 0.31, 0.86 MPa at 12 weeks ($P < 0.05$). The mean ultimate load to failure in the control, SN injury (+), and SN injury (−) groups were 17.37, 6.98, and 12.23 N at 4 weeks ($P < 0.05$); 17.69, 3.98, and 17.36 N at 8 weeks ($P < 0.05$); and 21.7, 7.13, and 18.99 N at 12 weeks ($P < 0.05$), respectively. The linear stiffness was 13.65, 3.98, and 2.33 N/mm^2 ($P < 0.05$) at 4 weeks; 18.14, 2.48, and 6.38 N/mm^2 at 8 weeks ($P < 0.05$); and 15.81, 2.23, 6.55 N/mm^2 at 12 weeks ($P < 0.05$). The mean Young's modulus was 7.79, 1.05, and 2.79 MPa at 4 weeks ($P < 0.05$); 8.63, 1.34, and 3.62 MPa at 8 weeks ($P < 0.05$); and 4.20, 1.72, and 2.85 MPa at 12 weeks ($P < 0.05$). Thus, there were significant differences between the groups at all time points after surgery (Fig. 8).

DISCUSSION

The present study evaluated alterations in both muscle and ten-

https://doi.org/10.5397/cise.2022.01207

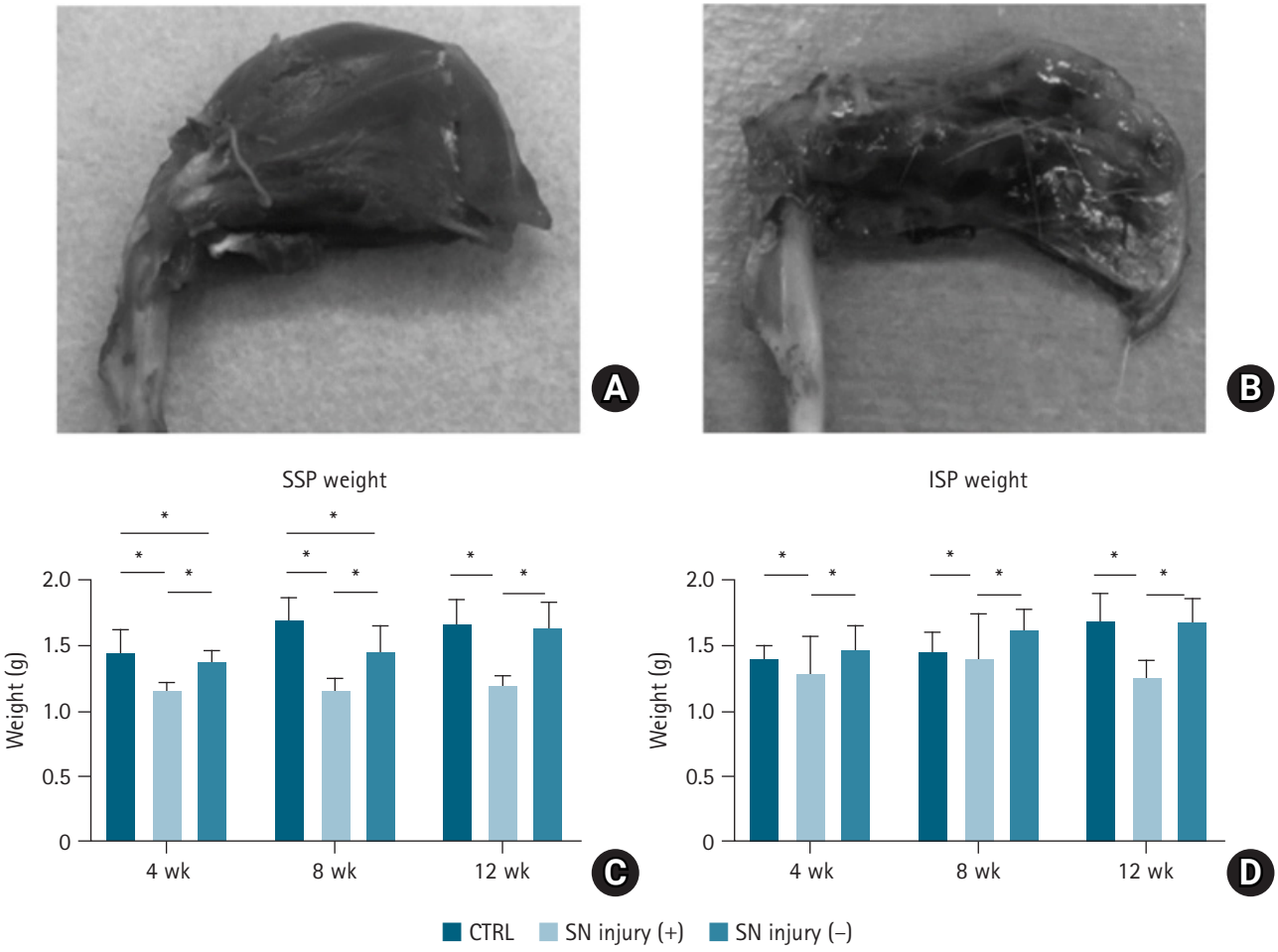

Fig. 3. The macroscopic appearance of muscles. (A) Image of the supraspinatus (SSP) and infraspinatus (ISP) muscles in the suprascapular nerve (SN) injury (–) group. (B) Image of the SSP and ISP muscles in the SN injury (+) group, exhibiting apparent atrophic changes. (C) Comparison of the SSP weight in the SN injury (+)/(–) groups and control (CTRL). (D) Comparison of the ISP weight in the SN injury (+)/(–) groups and CTRL. Error bars represent the standard deviation. *Significant difference (P<0.05).

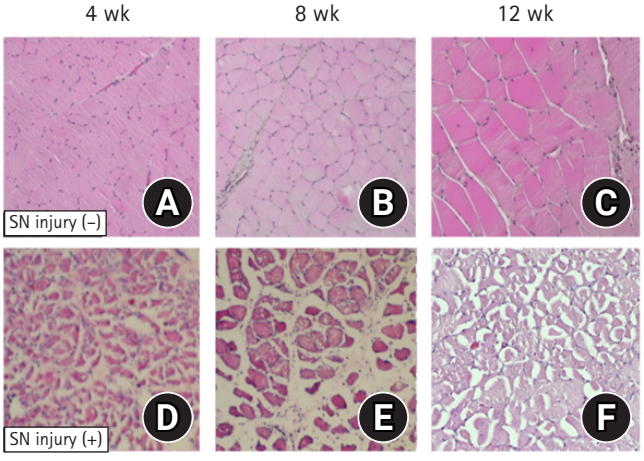

Fig. 4. Histological findings (H&E; magnification, ×100). (A-C) Suprascapular nerve (SN) injury (–) group. (D-F) SN injury (+) group.

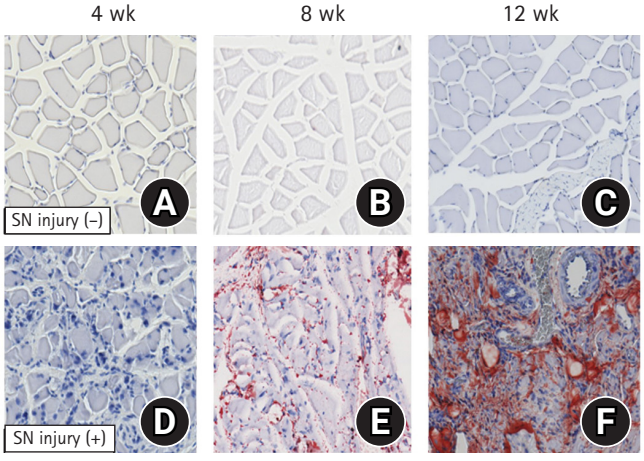

Fig. 5. Histological findings by Oil Red O stain (magnification, ×100). (A-C) Suprascapular nerve (SN) injury (–) group. (D-F) SN injury (+) group.

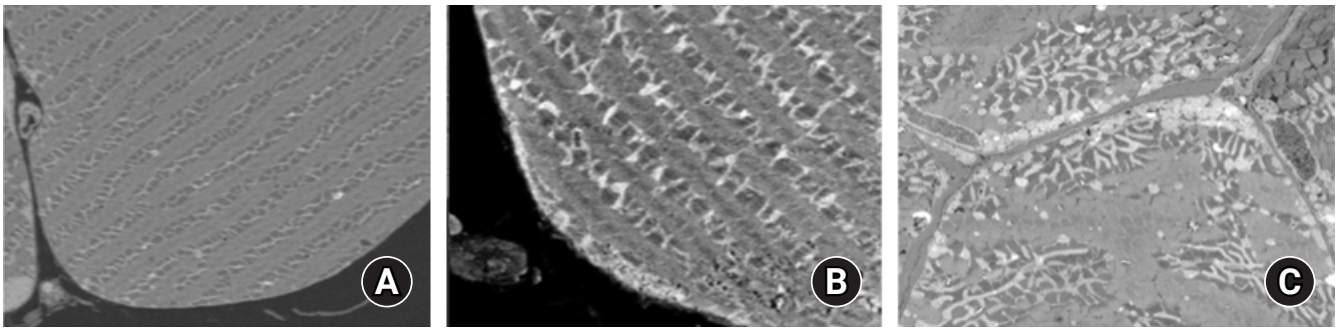

Fig. 6. Ultrastructural analysis. Single-section imaging via electron microscopy (magnification, ×2,000). (A) Control group. (B) Suprascapular nerve (SN) injury (–) group. (C) SN injury (+) group.

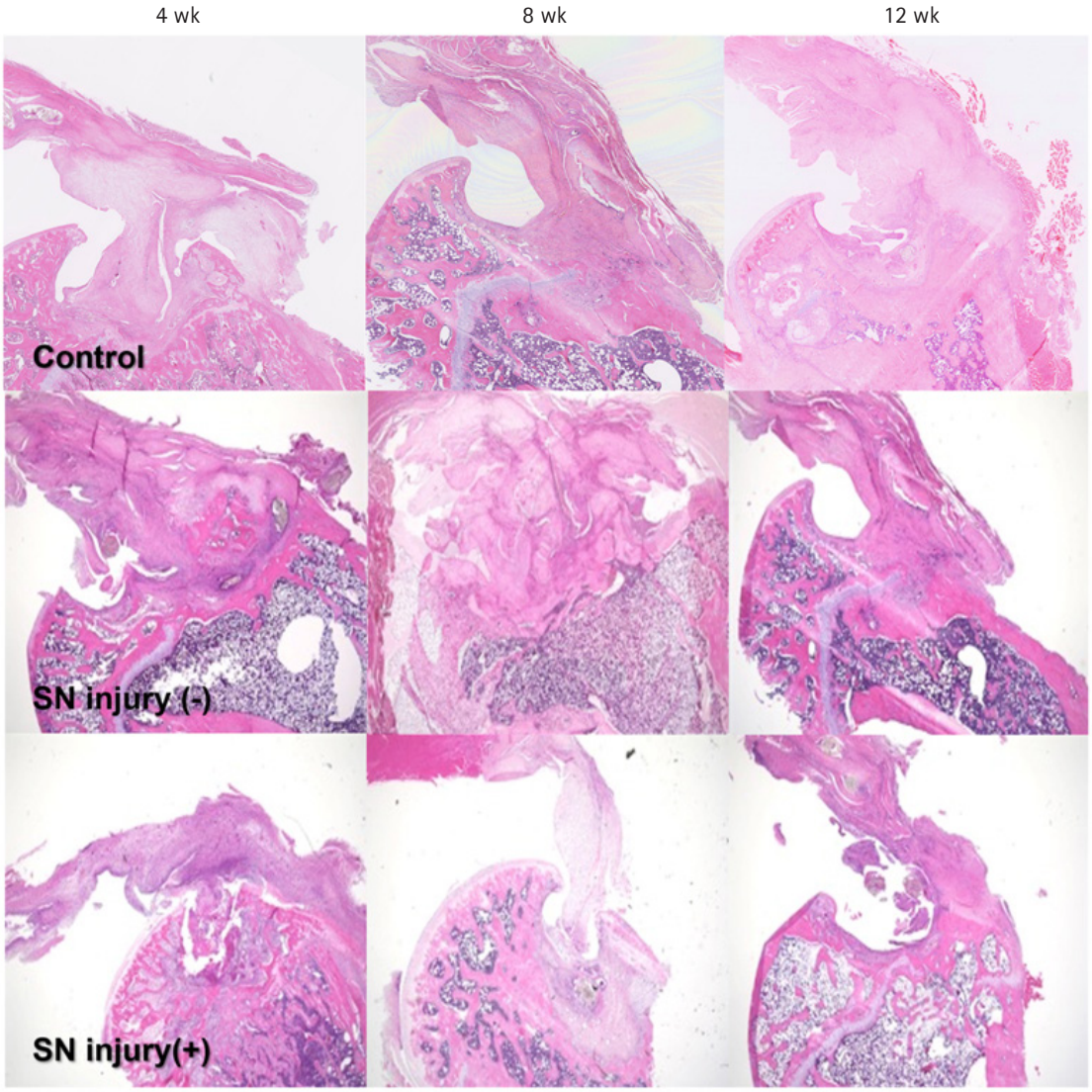

Fig. 7. Histological findings of the enthesis (H&E; magnification, ×100). SN: suprascapular nerve.

https://doi.org/10.5397/cise.2022.01207

don–bone insertion after SN injury in a massive RCT rat model. The SSP was relatively atrophic and there was more fat accumulation in the group with nerve injury compared to that without nerve injury. Ultrastructural analysis demonstrated that mitochondrial damage was relatively severe in the nerve-injured muscle. Interestingly, the regenerated tendon–bone insertion in the group with nerve injury was significantly immature in terms of both histological and biomechanical aspects. To the best of our knowledge, no previous studies have reported such data.

There have been some preliminary reports evaluating the influence of nerve injury on RC muscles. Liu et al. [15] reported that significant and consistent muscle atrophy occurred in a massive RCT rat model after SN transection. In their study, the SSP/ISP lost 25.4% and 28.9% of their wet weight, respectively, at 2 weeks after surgery, and 13.2% and 28.3%, respectively, at 6 weeks after surgery. Sasaki et al. [14] examined SSP changes in a massive tear rat model with or without SN nerve injury and reported two types of atrophy: myogenic atrophy in the group without nerve injury and neurogenic atrophy in the group with nerve injury. The present study reported similar RC muscle changes and mitochondrial damage at the ultrastructural level.

Previous studies have indicated a significant association between SN injuries and RC muscle fatty degeneration [14,19], concurring with the data of the present study. However, in clinical settings, these associations remain unclear. Costouros et al. [20] reported that the SN is damaged in a significant proportion of patients with massive RCTs, and they observed that seven of 26 massive RCT patients (38%) had isolated SN injury. Mallon et al. [21] reported that eight patients (100%) presenting with massive RCTs had SN neuropathy in the SSP and/or ISP muscles as revealed by electromyography. Meanwhile, Collin et al. [22] reported that six of 49 shoulders (12%) with massive RCTs had neurologic lesions on electromyography; however, they did not detect an SN lesion in the majority of massive RCT cases, and there was no association between neuropathy and massive RCT.

Elsewhere, a cadaveric study reported the effects of RCT retraction on the SN and concluded that SSP retraction dramatical-

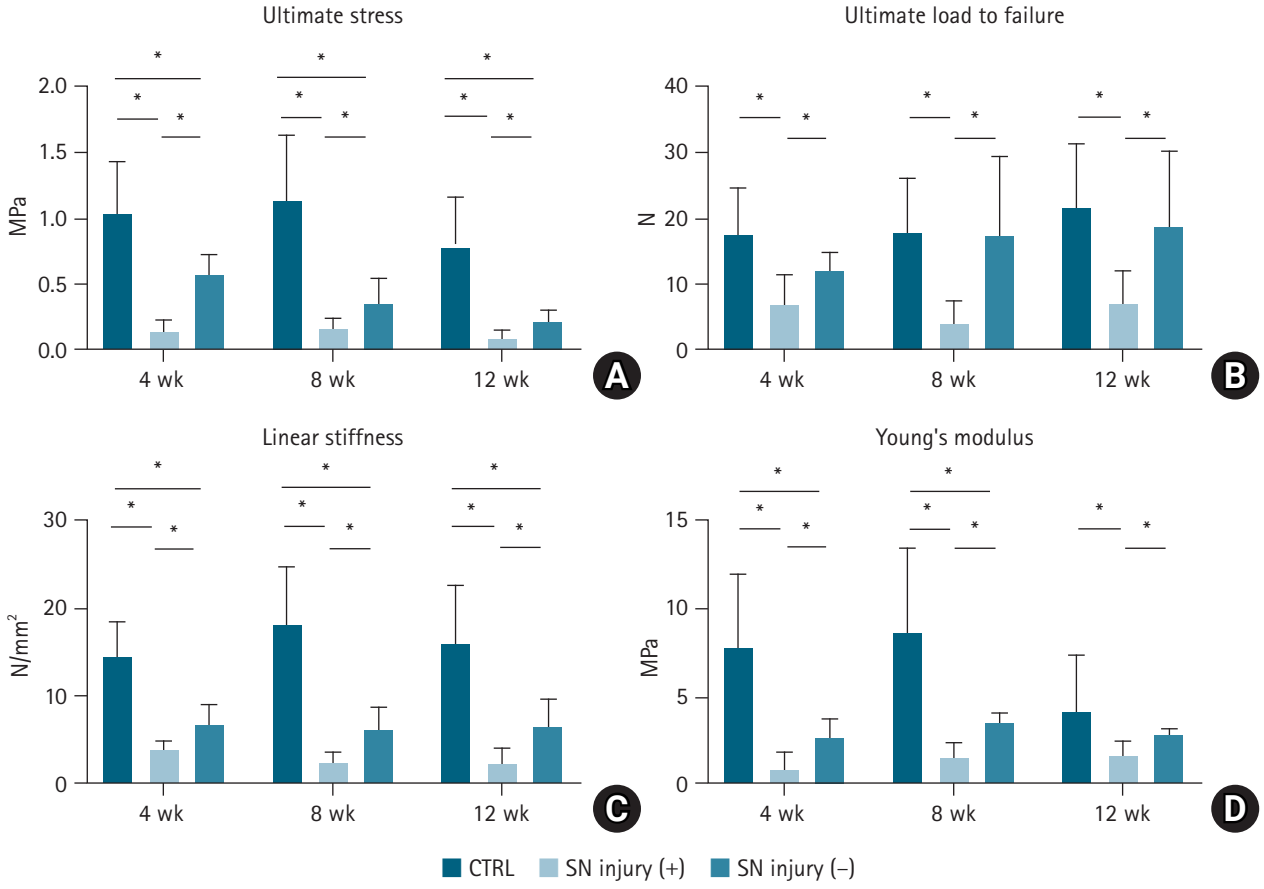

Fig. 8. Mechanical properties of muscles. (A) Ultimate stress. (B) Ultimate load to failure. (C) Linear stiffness. (D) Young's modulus. There are significant differences between the suprascapular nerve (SN) injury (+) and SN injury (–) groups for every item of mechanical testing at all time points. CTRL: control. *P<0.05.

ly changed its course, leading to kinking of the nerve. Shi et al. [13] reported that SN neuropathy correlates with tendon tear size but not fatty degeneration. Considering the fact that fatty degeneration does not affect SN myelination, they concluded that there might have been underdiagnosed cases in prior studies using electromyography/nerve conduction velocity [13]. This may explain the discrepancy between the basic/clinical studies regarding the association between SN injury and RCTs, thus indicating the possibility that SN injury is more significantly associated with this disease than is generally believed.

Gereli et al. [23] examined SSP and ISP enthesis morphometry in a rat model of SN transection without RCT. There was a significant decrease in cellularity (fibroblasts, collagen bundle diameter, and osteoblasts) in the tendon and bone at all time points. These changes eventually impaired enthesis healing by reducing the cellularity at all entheseal zones and diminishing the collagen bundle in the tendon zone. In fact, this study indicated that SN injury could affect the healing capacity in RCT, although the researchers did not conduct a biomechanical evaluation. The present study evaluated the alteration in terms of both aspects and found that histological changes were similar to those described above, while biomechanical properties were weakened at the denervated enthesis. These results suggest that SN denervation leads not only to histological immaturity but also structural weakness at the regenerated enthesis in RCT.

In studies using RCT models, the "detachment and repair" model is usually preferred. The present study used a "resection and detachment" model to confirm the effect of large tears with or without SSN injury on fatty degeneration and the granulation mutuality at the regenerated enthesis. Unlike in humans, in rats, the defect is gradually covered by granulation tissue. Given that the data show that denervation inhibits enthesis regeneration via the surrounding tissue, which is non-innervated by the SS nerve, it stands to reason there would be an inhibitory effect of SSN injury on tendon healing in RC repair.

There were several limitations to this study. First, the anatomy and function of rat shoulders differ from those of human shoulders. In particular, the acromial arch in quadrupedal animals is different as it involves reduced coverage of the subscapularis compared to bipedal animals. Second, the SN injury model was made by nerve dissection according to previous studies [15,23,24], whereas, in a clinical setting, SN injury is caused by SSP retraction after RC tearing [16]. Finally, the present study used the Mann-Whitney U-test adjusted by the Holm-Bonferroni test for statistical analysis. Although we believe our statistical analysis was valid, the power level of the analysis may have been relatively low compared to that attainable with the Kruskal-Wallis test with further adjustment. Further analysis of these concerns will refine the data obtained from this study.

CONCLUSIONS

The present study evaluated muscle and entheseal change in large tears with or without SSN injury in a rat model. In rats with nerve injury, marked muscle fatty degeneration was seen and the regenerated enthesis was relatively immature compared to in the rats without injury. In terms of clinical relevance, these results may indicate that SN injury leads not only to severe fatty changes in large RCTs but also to the inhibition of tendon healing after surgery.

NOTES

ORCID

Hiroki Ohzon https://orcid.org/0000-0001-7170-5401

Author contributions

Conceptualization: KE, MG, HS. Data curation: KE, KT, TK. Formal Analysis: KE, TK. Investigation: KE, HS, HN. Methodology: KE, HN. Project administration: KE, HO, MG, HS. Resources: KE. Supervision: KE, TO, NS. Validation: KE, HO, MG, HN, TO, NS. Visualization: KE, TK. Writing – original draft: KE, HO, MG. Writing – review & editing: KE, MG.

Conflict of interest

None.

Funding

None.

Data availability

Contact the corresponding author for data availability.

Acknowledgments

None.

REFERENCES

1. McElvany MD, McGoldrick E, Gee AO, Neradilek MB, Matsen FA 3rd. Rotator cuff repair: published evidence on factors associated with repair integrity and clinical outcome. Am J Sports Med 2015;43:491–500.
2. Galatz LM, Ball CM, Teefey SA, Middleton WD, Yamaguchi K. The outcome and repair integrity of completely arthroscopically

https://doi.org/10.5397/cise.2022.01207

repaired large and massive rotator cuff tears. J Bone Joint Surg Am 2004;86:219–24.
3. Lädermann A, Denard PJ, Collin P. Massive rotator cuff tears: definition and treatment. Int Orthop 2015;39:2403–14.
4. Choi S, Kim MK, Kim GM, Roh YH, Hwang IK, Kang H. Factors associated with clinical and structural outcomes after arthroscopic rotator cuff repair with a suture bridge technique in medium, large, and massive tears. J Shoulder Elbow Surg 2014;23:1675–81.
5. Chillemi C, Petrozza V, Garro L, et al. Rotator cuff re-tear or non-healing: histopathological aspects and predictive factors. Knee Surg Sports Traumatol Arthrosc 2011;19:1588–96.
6. Mall NA, Tanaka MJ, Choi LS, Paletta GA Jr. Factors affecting rotator cuff healing. J Bone Joint Surg Am 2014;96:778–88.
7. Matsumoto F, Uhthoff HK, Trudel G, Loehr JF. Delayed tendon reattachment does not reverse atrophy and fat accumulation of the supraspinatus: an experimental study in rabbits. J Orthop Res 2002;20:357–63.
8. Uhthoff HK, Coletta E, Trudel G. Intramuscular fat accumulation and muscle atrophy in the absence of muscle retraction. Bone Joint Res 2014;3:117–22.
9. Gerber C, Fuchs B, Hodler J. The results of repair of massive tears of the rotator cuff. J Bone Joint Surg Am 2000;82:505–15.
10. Goutallier D, Postel JM, Bernageau J, Lavau L, Voisin MC. Fatty muscle degeneration in cuff ruptures: pre- and postoperative evaluation by CT scan. Clin Orthop Relat Res 1994;(304):78–83.
11. Thomazeau H, Boukobza E, Morcet N, Chaperon J, Langlais F. Prediction of rotator cuff repair results by magnetic resonance imaging. Clin Orthop Relat Res 1997;(344):275–83.
12. Lafosse L, Brozska R, Toussaint B, Gobezie R. The outcome and structural integrity of arthroscopic rotator cuff repair with use of the double-row suture anchor technique. J Bone Joint Surg Am 2007;89:1533–41.
13. Shi LL, Boykin RE, Lin A, Warner JJ. Association of suprascapular neuropathy with rotator cuff tendon tears and fatty degeneration. J Shoulder Elbow Surg 2014;23:339–46.
14. Sasaki Y, Ochiai N, Hashimoto E, et al. Relationship between neuropathy proximal to the suprascapular nerve and rotator cuff tear in a rodent model. J Orthop Sci 2018;23:414–9.
15. Liu X, Manzano G, Kim HT, Feeley BT. A rat model of massive rotator cuff tears. J Orthop Res 2011;29:588–95.
16. Albritton MJ, Graham RD, Richards RS 2nd, Basamania CJ. An anatomic study of the effects on the suprascapular nerve due to retraction of the supraspinatus muscle after a rotator cuff tear. J Shoulder Elbow Surg 2003;12:497–500.
17. Kanazawa T, Gotoh M, Ohta K, et al. Histomorphometric and ultrastructural analysis of the tendon-bone interface after rotator cuff repair in a rat model. Sci Rep 2016;6:33800.
18. Nakamura H, Gotoh M, Kanazawa T, et al. Effects of corticosteroids and hyaluronic acid on torn rotator cuff tendons in vitro and in rats. J Orthop Res 2015;33:1523–30.
19. Wang Z, Feeley BT, Kim HT, Liu X. Reversal of fatty infiltration after suprascapular nerve compression release is dependent on UCP1 expression in mice. Clin Orthop Relat Res 2018;476:1665–79.
20. Costouros JG, Porramatikul M, Lie DT, Warner JJ. Reversal of suprascapular neuropathy following arthroscopic repair of massive supraspinatus and infraspinatus rotator cuff tears. Arthroscopy 2007;23:1152–61.
21. Mallon WJ, Wilson RJ, Basamania CJ. The association of suprascapular neuropathy with massive rotator cuff tears: a preliminary report. J Shoulder Elbow Surg 2006;15:395–8.
22. Collin P, Treseder T, Lädermann A, et al. Neuropathy of the suprascapular nerve and massive rotator cuff tears: a prospective electromyographic study. J Shoulder Elbow Surg 2014;23:28–34.
23. Gereli A, Uslu S, Okur B, Ulku TK, Kocaoğlu B, Yoo YS. Effect of suprascapular nerve injury on rotator cuff enthesis. J Shoulder Elbow Surg 2020;29:1584–9.
24. Kim HM, Galatz LM, Lim C, Havlioglu N, Thomopoulos S. The effect of tear size and nerve injury on rotator cuff muscle fatty degeneration in a rodent animal model. J Shoulder Elbow Surg 2012;21:847–58.